LAMINAR HEAT TRANSFER IN A MOVING BED CHANNEL USING A TWO ENERGY EQUATION MODEL

Ana Cristina Pivem, anapivem@ita.br
Marcelo J.S. de Lemos, delemos@ita.br
Departamento de Energia, IEME, Instituto Tecnológico de Aeronáutica - ITA

Abstract. *The objective of this work is to present simulations for laminar heat transfer in a porous reactor, in which both the permeable bed and the working fluid moves with respect to the fixed bounding walls. For simulating the flow and heat transfer, a two-energy equation model is applied in addition to a mechanical model. Transport equations are discretized using the control-volume method and the system of algebraic equations are relaxed via the SIMPLE algorithm. The effects of solid-to-fluid thermal conductivity and solid-to-fluid ratio of thermal capacity are analyzed.*

Keywords*: moving bed, porous media, heat transfer*

1. INTRODUCTION

There is an increasing interest in the use of moving bed technology as the separation of chemical compounds, recuperation of petrochemical processes, drying of grains and seeds, removal of organic matter in the affluent by means of a moving bed, etc. The advantages of using a moving bed are low investment, low energy consumption, low maintenance and improvement process performance, such as reducing the moisture content in agricultural products, for example. Another important technology that can benefit from the studies herein is a moving bed composed of pellets. Pellet techniques are used for various purposes, among them one can mention the pelletization of iron ore for steel making and use of biomass for energy production.

With respect to pelletization of iron ore, Parisi and Laborde (2004) and Negri et.al. (1991) presented a study about the direct reduction of iron oxide in a countercurrent reactor in a moving bed. Also within this context, Valipour et.al.(2006) developed a mathematical model to simulate grain kinetics and thermal behavior of a pellet of porous iron oxide. Their study considered chemical reactions with a mixture of hydrogen, carbon monoxide, carbon dioxide and water vapor. Further, Valipour and Saboohi (2007a) presented a mathematical model to simulate the multiple heterogeneous reactions occurring in a moving bed of porous pellets in a reactor. Valipour and Saboohi (2007b) described a model to predict countercurrent flow in a cylindrical reactor in which pellets of iron ore went through a gas mixture.

Henda and Falcioni (2006) described the thermal performance of a pre-heater that consists of a moving bed of pellets of nickel in concurrent flow with a gas, using both one and two equations energy models. Nakayama and Kuwahara et.al. (2001) presented the exact solution of energy equations for two fundamental cases, i.e. one-dimensional porous plate with internal heat generation within the solid and, as a second case, the thermally developing unidirectional flow through a semi-infinite porous medium.

The present study is concerned with simulation of energy transport in a moving bed though which a laminar flow occurs. Energy equations for both phases are applied.

2. MACROSCOPIC MODEL FOR FLOW EQUATIONS

2.1. Fixed Bed

A macroscopic form of the governing equations is obtained by taking the volumetric average of the entire equation set. In this development, the porous medium is considered to be rigid, fixed and saturated by the incompressible fluid. Derivation of this equation set is already available in the literature, Pedras and de Lemos (2001a), Pedras and de Lemos (2001b) and de Lemos (2006), so that details need not to be repeated here. Nevertheless, for the sake of completeness, the final laminar incompressible form of the equations is here presented:

Continuity:

$$\nabla \cdot \mathbf{u}_D = 0 \tag{1}$$

Momentum:

$$\rho\left[\frac{\partial \mathbf{u}_D}{\partial t} + \nabla \cdot \left(\frac{\mathbf{u}_D \mathbf{u}_D}{\phi}\right)\right] = -\nabla(\phi \langle \overline{p} \rangle^i) + \mu \nabla^2 \mathbf{u}_D - \left[\frac{\mu \phi}{K}\mathbf{u}_D + \frac{c_F \phi \rho |\mathbf{u}_D| \mathbf{u}_D}{\sqrt{K}}\right] \tag{2}$$

where the last two terms in Eq.(2) represent the Darcy and Forchheimer contributions. The symbol K is the porous medium permeability, c_F is the form drag or Forchheimer coefficient, $\langle \overline{p} \rangle^i$ is the intrinsic average pressure of the fluid, $\mathbf{u}_D$ is the Darcy velocity vector, ρ is the density, μ is the fluid dynamic viscosity and ϕ is the porosity of the porous medium.

2.2. Moving Bed

For a moving bed, only cases where the solid phase velocity is kept constant will be considered here, or say, we consider here a moving bed that crosses a fixed control volume in addition to a flowing fluid, which is not necessarily moving with a velocity aligned with the solid phase velocity. The steps below show first some basic definitions prior to presenting a proposal for a set of transport equations for analyzing such systems.

A general form for a volume-average of any property φ, distributed within a phase γ that occupy volume ΔV_γ, can be written as Gray and Lee (1977) ,

$$\langle \varphi \rangle^\gamma = \frac{1}{\Delta V_\gamma} \int_{\Delta V_\gamma} \varphi \, dV_\gamma \tag{3}$$

In the general case, the volume ratio occupied by phase γ will be $\phi^\gamma = \Delta V_\gamma / \Delta V$.

If there are two phases, a solid $\gamma = s$ and a fluid phase $\gamma = f$, volume average can be established on both regions. Also,

$$\phi^s = \Delta V_s / \Delta V = 1 - \Delta V_f / \Delta V = 1 - \phi^f \tag{4}$$

and for simplicity of notation one can drop the superscript "*f*" to get $\phi^s = 1 - \phi$.

As such, calling the instantaneous local velocities for the solid and fluid phases, $\mathbf{u}_s$ and $\mathbf{u}$, respectively, one can obtain the average for the solid velocity, within the solid phase, as follows,

$$\langle \mathbf{u} \rangle^s = \frac{1}{\Delta V_s} \int_{\Delta V_s} \mathbf{u}_s \, dV_s \tag{5}$$

with, in turn, can be related to an average velocity referent to the entire REV as,

$$\mathbf{u}_s = \frac{\overbrace{\Delta V_s}^{(1-\phi)}}{\Delta V} \underbrace{\frac{1}{\Delta V_s} \int_{\Delta V_s} \mathbf{u}_s \, dV_s}_{\langle \mathbf{u} \rangle^S} \tag{6}$$

A further approximation herein is that the porous bed is kept rigid and moves with a steady average velocity $\mathbf{u}_s$.

For the fluid phase, the intrinsic (fluid) volume average gives, after using the subscript "*i*" also for consistency with the literature,

$$\langle \mathbf{u} \rangle^i = \frac{1}{\Delta V_f} \int_{\Delta V_f} \mathbf{u} \, dV_f \tag{7}$$

Both velocities can then be written as,

$$\mathbf{u}_D = \phi \langle \mathbf{u} \rangle^i \, , \; \mathbf{u}_s = (1-\phi) \langle \mathbf{u} \rangle^s = const \, . \tag{8}$$

A relative velocity is then defined as,

$$\mathbf{u}_{rel} = \mathbf{u}_D - \mathbf{u}_s \tag{9}$$

Assuming that the relative movement between the two phases is macroscopically described by Eq. (9), the momentum equation reads,

$$\rho\left[\frac{\partial \mathbf{u}_D}{\partial t}+\nabla\cdot\left(\frac{\mathbf{u}_D\mathbf{u}_D}{\phi}\right)\right]=-\nabla(\phi\langle\bar{p}\rangle^i)+\mu\nabla^2\mathbf{u}_D-\underbrace{\left[\frac{\mu\phi}{K}\mathbf{u}_{rel}+\frac{c_F\phi\rho|\mathbf{u}_{rel}|\,\mathbf{u}_{rel}}{\sqrt{K}}\right]}_{relative\ drag} \tag{10}$$

Temperatures for the fluid and solid phase are governed by,

$$\left\{\left(\rho c_p\right)_f\phi\right\}\frac{\partial\langle T_f\rangle^i}{\partial t}+\left(\rho c_p\right)_f\nabla\cdot\left(\mathbf{u}_D\langle T_f\rangle^i\right)=\nabla\cdot\left\{\mathbf{K}_{eff,f}\cdot\nabla\langle T_f\rangle^i\right\}+h_i a_i\left(\langle T_s\rangle^i-\langle T_f\rangle^i\right) \tag{11}$$

$$\left\{(1-\phi)\left(\rho c_p\right)_s\right\}\frac{\partial\langle T_s\rangle^i}{\partial t}+\left(\rho c_p\right)_s\nabla\cdot\left(\mathbf{u}_s\langle T_s\rangle^i\right)=\nabla\cdot\left\{\mathbf{K}_{eff,s}\cdot\nabla\langle T_s\rangle^i\right\}-h_i a_i\left(\langle T_s\rangle^i-\langle T_f\rangle^i\right) \tag{12}$$

where c_p is the specific heat, and $\left\langle T_f\right\rangle^i$, $\left\langle T_s\right\rangle^i$, $\mathbf{K}`s$, a_i and h_i are the fluid and solid temperatures, the conductive tensors, the interfacial area and interfacial heat transfer coefficient, respectively, see Saito and de Lemos (2006).

Non-dimensional temperatures for the solid and fluid are defined as:

$$\theta_{s,f}=\frac{\left\langle T_{s,f}\right\rangle^i-T_{\min}}{T_{\max}-T_{\min}} \tag{13}$$

where the subscripts s, f stands for the solid and fluid phases, respectively, and "max" and "min" refers to both temperature maximum and minimum of either phase.

As temperature values in the simulations are low, radiation heat transfer was not considered in the model.

3. NUMERICAL METHOD

The equations set above, subjected to the interface and boundary conditions, were discretized in a two-dimensional control volume involving both clear and porous media. The finite volume method was used in the discretization and the SIMPLE algorithm Patankar (1980) was used to the handle the pressure-velocity coupling.

Figure 1 presents a typical control volume written in the generalized coordinates system $\eta-\xi$. The discretized form of the two-dimensional conservation equation for a generic property φ, in permanent regime, is given by:

$$I_e+I_w+I_n+I_s=S_\varphi \tag{14}$$

where I_e, I_w, I_n and I_s represent, respectively, the fluxes of φ in the faces east, west, north and south of the control volume and S_φ its source term.

Standard source term linearization is accomplished by using,

$$S_\varphi\approx S_\varphi^{**}\langle\varphi\rangle_p^i+S_\varphi^* \tag{15}$$

Discretization of the momentum equation in the *x*-direction gives,

$$S^{*x}=\left(S_e^{*x}\right)_P-\left(S_w^{*x}\right)_P+\left(S_n^{*x}\right)_P-\left(S_s^{*x}\right)_P+S_P^* \tag{16}$$

$$S^{**x}=S_\phi^{**} \tag{17}$$

where, S^{*x} is the diffusive part, here treated in an explicit form. The second term, S^{**x}, entails the additional drag forces due to the porous matrix, which are here treated explicitly.

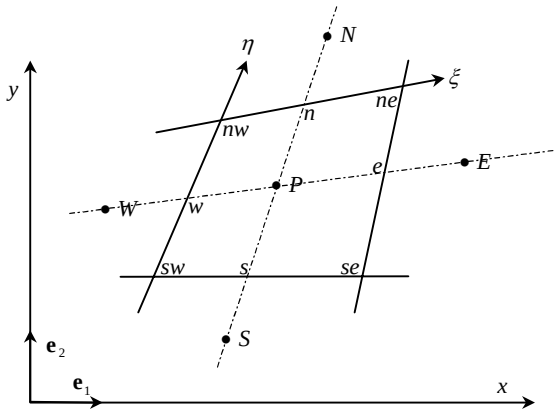

Figure 1: Control volume and notation

3.1. Boundary Conditions

A numerical example using the above presented model is shown next. The flow under consideration is schematically presented in Figure 2, where a channel is completely filled with a moving layer of a porous material. The channel shown in the figure has length and height given by *L* and *H*, respectively. A constant property fluid flows longitudinally from left to right permeating through the porous structure. Both walls are kept isolated and the fluid and solid are given a different temperature at the inlet.

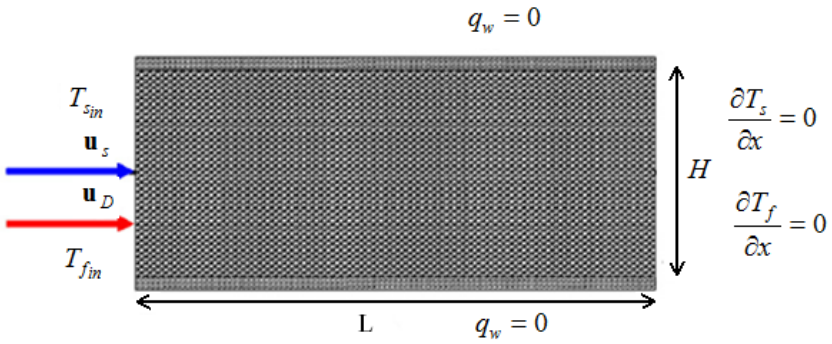

Figure 2. Porous bed reactor with a moving solid matrix.

Boundary conditions are given by:

On the solid walls:

$$\langle \mathbf{u} \rangle^i = 0 \,,\; q_w = 0 \tag{18}$$

At entrance:

$$\mathbf{u}_D = \mathbf{u}_{inlet} \,,\; \langle T_f \rangle^i = T^f_{inlet} \,,\; \langle T_s \rangle^i = T^s_{inlet} \,. \tag{19}$$

4. RESULTS AND DISCUSION

The following simulations analyze the effect of thermal capacity ratio, $(\rho c_p)_s / (\rho c_p)_f$, and the effect of thermal conductivity ratio, k_s / k_f, on temperature profiles for a fixed velocity ratio u_s / u_D in concurrent laminar flow.

The used properties of solid and fluid are presented in Table 1.

Table 1. Physical properties of solid and fluid used in Eqns.(11) and (12).

Fluid: Water Vapour				
$k_f(W/mK)$	$\rho_f(kg/m^3)$	$c_{ps}(J/kgK)$	$\mu(Ns/m^2)$	$T(K)$
0.0345	0.4345	1986.8	173.1×10^{-7}	507.5
Solid: Silicon Dioxide				
$k_s(W/mK)$	$\rho_s(kg/m^3)$	$c_{ps}(J/kgK)$	-	$T(K)$
1.38	2220	745	-	300

4.1. Effect of thermal capacity ratio $(\rho c_p)_s/(\rho c_p)_f$

The effects of Reynolds number $Re_D = \dfrac{\rho|\mathbf{u}_{rel}|D}{\mu}$, slip ratio $\mathbf{u}_s/\mathbf{u}_D$ and Darcy number $Da = K/H^2$, where $K = \dfrac{D^2\phi^2}{144(1-\phi)^2}$ and D is the particle diameter, have been analyzed in Pivem and de Lemos (2010) and for that they are here not repeated.

Figure 3 shows the effect of the thermal capacity ratio on dimensionless temperature distributions along the axial direction. The density and specific heat of the fluid are kept constant and are given by $\rho = 0.4345 kg/m^3$ and $(c_p)_f = 1986.8\ J/kg\,K$, respectively. It is observed in Figure 3 that increasing the thermal capacity of the solid, $(\rho c_p)_s$, the equilibrium temperature tends to approach the inlet temperature of the solid, or say, for higher values of $(\rho c_p)_s$, more energy exchange is needed to vary the temperature of the solid by a certain amount.

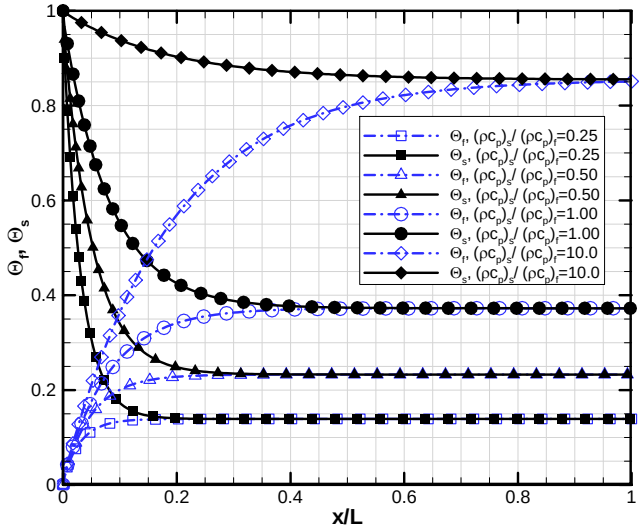

Figure 3 - Non-dimensional temperatures as a function of $(\rho c_p)_s/(\rho c_p)_f$, with $u_s/u_D = 0.5$, $k_s/k_f = 25$, $\phi = 0.9$, $Da = 1{,}498\times10^{-3}$, $Re_D = 20$.

4.2. Effect of thermal conductivity ratio k_s/k_f

Figure 4a shows the effect of k_s / k_f on longitudinal non-dimensional temperatures. It is noted that the higher the ratio k_s / k_f, the longer is the length needed for thermal development since heat is transported only by conduction within the solid, which causes its temperature distribution to be more connected to the inlet temperature.

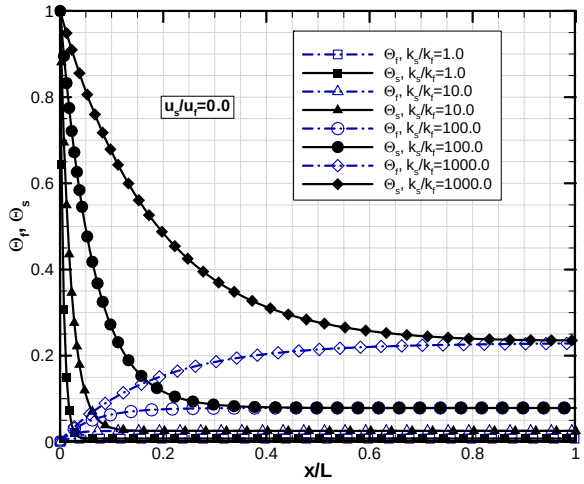

a)

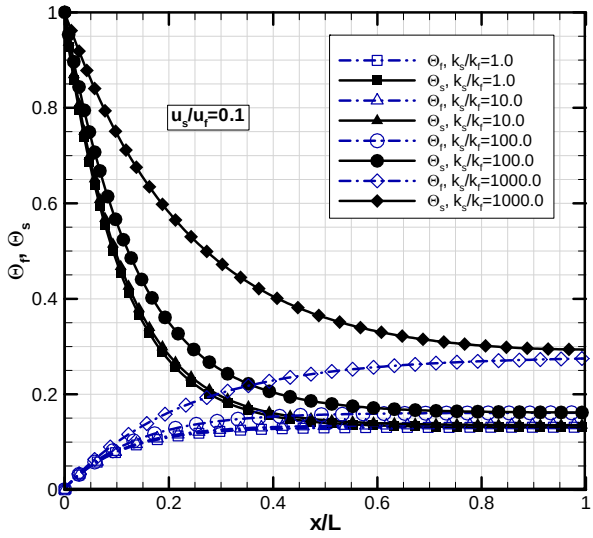

b)

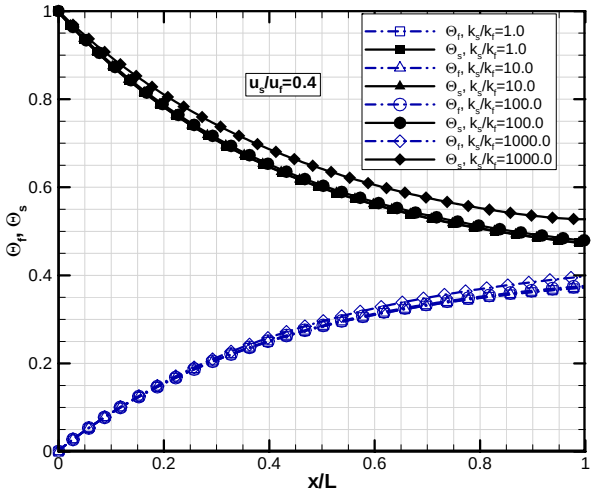

c)

Figure 4: a), b), c) - Non-dimensional temperatures as a function of k_s / k_f, with

$$\phi = 0.6\,,\ Da = 4.162\times10^{-3}\,,\ (\rho c_p)_s/(\rho c_p)_f = 1.5\,.$$

With increasing k_s/k_f, (Figure 4b) higher solid temperatures increase the equilibrium temperature of the system. On the other hand, by decreasing the thermal conductivity ratio k_s/k_f, a shorter axial length is needed for the equilibrium temperature to be reached.

Note also that for $u_s/u_D = 0$ (Figure 4a), the variation in the ratio of thermal conductivity leads to a minimum change in equilibrium temperature along the channel in comparison with results for moving beds (Figs. 4b and 4c).

For $u_s/u_D = 0.4$ (Figure 4c), the ratio of thermal conductivity causes little influence on the temperature distribution within each phase along the channel. For high solid mass flow rates, with u_s/u_D approaching to 1, exchange of heat between phases occurs mostly by conduction, leading to longer developing lengths.

5. CONCLUSIONS

This paper investigated the behavior of a two-energy equation model to simulate flow and heat transfer in a moving porous bed. Numerical solutions for laminar flow in a moving bed porous were obtained for different ratio of thermal capacity $(\rho c_p)_s/(\rho c_p)_f$ and of ratio of thermal conductivity k_s/k_f, varying the slip ratio $\mathbf{u}_s/\mathbf{u}_D$. Governing equations were discretized and numerically solved. The following conclusions were observed:

For low values of $\mathbf{u}_s/\mathbf{u}_D$, $(\rho c_p)_s/(\rho c_p)_f$ and k_s/k_f, thermal equilibrium between phases require smaller axial lengths. Increasing the speed of the solid relative to the fluid speed reduces the interfacial drag forces and the transport of energy between the phases is mainly due to conduction.

The results presented here have a wide application to problems involving engineering equipment that could be identified as a moving bed porous.

6. ACKNOWLEDGEMENTS

The authors are thankful to CNPq, Brazil, for their financial support during the course of this research.

7. REFERENCES

de Lemos M.J.S., 2006, Turbulence in Porous Media: Modeling and Applications, Elsevier, Amsterdam.

de Lemos M.J.S, Saito M.B., 2008, Computation of turbulent heat transfer in a moving porous bed using a macroscopic two-energy equation model, International, Communications in Heat and Mass Transfer 35 1262–1266.

Gray W.G., Lee P.C.Y., 1977 , On the theorems for local volume averaging of multiphase system, International Journal of Multiphase Flow 3 333–340.

Henda R, Falcioni D.J., 2006, Modeling of heat transfer in a moving packed bed: Case of the preheater in nickel carbonyl process, JOURNAL OF APPLIED MECHANICS –ASME, Vol. 73(1), pp. 47-53.

Nakayama A., Kuwahara F., Sugiyama M., Xu G., 2001 , "A two energy equation model for conduction and convection in porous media", International Journal of Heat and Mass Transfer, Vol. 44, pp. 4375 – 4379.

Negri E. D., Alfano O. M., Chiovetta M. G., 1991, Direct Redution of Hematite in a Moving-Bed Reactor: Analysis of the Water Gas Shift Reaction Effects on the Reactor Behavior, American Chemical Society, Vol. 30, pp. 474-482.

Parisi, D.R., Laborde, M.A., 2004, Modeling of counter current moving bed gas-solid reactor used in direct reduction of iron ore, Chemical Engineering Journal, 104, 35-43.

Pedras, M.H.J., de Lemos, M.J.S., 2001a, Macroscopic Turbulence Modeling for Incompressible Flow Through Undeformable Porous Media, Intern. J. Heat and Mass Transfer, vol. 44, n. 6, pp. 1081-1093.

Pedras, M.H.J., de Lemos, M.J.S., 2001b, Simulation of Turbulent Flow in Porous Media Using a Spatially Periodic Array and a Low Re Two-Equation Closure, Numerical Heat Transfer - Part A Applications, vol. 39, n. 1, pp. 35-39.

Pivem, A. C, de Lemos, M. J. S., 2010, "Heat transfer in a moving porous bed using a two-energy equation closure", CONEM 2010, VI Congresso Nacional de Engenharia Mecânica, Agosto 18-21, Campina Grande-PB.

Saito M.B., de Lemos M.J.S., 2005, "Interfacial heat transfer coefficient for non-equilibrium convective transport in porous media", International Communications in Heat and Mass Transfer, Vol. 32 (5), pp. 667–677.

Saito M.B., de Lemos M.J.S., 2006 , "A correlation for interfacial heat transfer coefficient for turbulent flow over an array of square rods", Journal of Heat Transfer, Vol. 128, pp. 444–452.

S.V. Patankar, Numerical Heat Transfer and Fluid Flow, Hemisphere, Washington, DC, (1980).

Valipour M.S., Hashemi M.Y.M., Saboohi Y., 2006, Mathematical modeling of the reaction in an iron ore pellet using a mixture of hydrogen, water vapor, carbon monoxide and carbon dioxide: an isothermal study, ADVANCED POWDER TECHNOLOGY, Vol. 17 (3), pp. 277-295.

Valipour M.S., Saboohi Y., 2007a, Numerical investigation of nonisothermal reduction hematite using Syngas: the shaft scale study, Modelling Simul. Mater. Sci. Eng., Vol. 15, pp. 487–507.

Valipour M.S., Saboohi Y., 2007b, Modeling of multiple noncatalytic gas-solid reactions in a moving bed of porous pellets based on finite volume method, HEAT AND MASS TRANSFER, Vol. 43 (9), pp. 881-894.